

LASERS

PACS numbers: 42.55.Lt; 42.60.Lh
DOI: 10.1070/QE2009v039n12ABEH014077

High-repetition-rate plate-electrode CO_2 laser

A.V. Andramanov, D.D. Voevodin, A.V. Vysotskii, S.A. Kabaev,
B.V. Lazhintsev, V.A. Nor-Arevyan, A.V. Pisetkaya, V.D. Selemir

***Abstract*. A high-repetition-rate CO_2 laser with the inductive-capacitive discharge stabilisation is studied for the first time. A multisection discharge gap of length 250 mm was formed by pairs of anode – cathode plates arranged in the form of a broken line. The width of the discharge region between each pair of the plates was ~ 1.3 mm and height ~ 12 mm. The cross section of the laser beam on the output mirror of the resonator was $\sim 6 \times 8$ mm. The maximum output energy of the laser using the $CO_2:N_2:He = 32:32:96$ Torr mixture was 15.9 mJ, the lasing efficiency being 1.7 %. For a relatively low gas flow rate of 19 m s^{-1}, a CO_2 laser pulse repetition rate of 3 kHz was achieved, the relative root-mean-square deviation of the pulse energy being within 5 %. The average output power of the laser was ~ 40 W.**

Keywords: *CO_2 laser, plate electrodes, inductive-capacitive stabilisation, pulse repetition rate, output energy stability, gas flow rate, energy parameters.*

1. Introduction

High-repetition-rate CO_2 lasers can be used in lidars and radars, for laser isotope separation, material processing, optical pumping of far-IR lasers, and lithography. Thus, a pulse repetition rate $f = 1.1$ kHz was achieved in a CO_2 laser [1] with a gas flow rate $v = 72$ m s^{-1} in the interelectrode gap and the discharge region of width $b = 2.5$ cm. For CO_2 lasers with a pulse repetition rate of a few kilohertz, the discharge region width is typically ~ 1 cm and the gas flow rate in the interelectrode gap is even higher. Thus, the laser studied in [2] had $f \leqslant 2$ kHz and $b \approx 1$ cm for $v \sim 100$ m s^{-1}.

The pulse repetition rate in well-studied excimer lasers pumped by a volume self-sustained discharge can be increased by considerably decreasing the discharge region width. The pulse repetition rate achieved in a massive-electrode KrF laser was 5 kHz for $v \sim 55$ m s^{-1} and the characteristic discharge region width ~ 0.3 cm [3]. The pulse repetition rate achieved in a multisection-plate-electrode XeF laser with the inductive-capacitive discharge stabilisation was $\leqslant 4.5$ kHz for $v \leqslant 19$ m s^{-1} and the characteristic discharge region width $b \sim 0.1$ cm [4]. The excitation of the active medium of CO_2 lasers by narrow discharges, as in [3, 4], will result in significant diffraction losses in the laser resonator because the emission wavelength of the CO_2 laser is considerably (30 – 50 times) longer that that of excimer lasers.

The active medium of a high-repetition-rate chemical HF (DF) laser was excited in [5] by using plate electrodes in conjunction with the inductive-capacitance discharge stabilisation. To reduce diffraction losses in the laser resonator, the anode – cathode plate pairs were located in planes making angle α with the optical axis. This approach was first proposed in [6]. For the gas flow rate $v \leqslant 19$ m s^{-1}, the pulse repetition rate $f = 2.4$ kHz was obtained.

In this paper, we present the results of the first experimental studies of a plate-electrode CO_2 laser with the inductive-capacitive discharge stabilisation and a high pulse repetition rate. The gas-circulation system in the standard operation regime of a diametric fan provided the gas-flow rate in the interelectrode gap up to 19 m s^{-1}.

2. Experimental results

The CO_2 laser was assembled based on a serial CL-5000 laser chamber [5] and a new electrode unit with a multisection discharge gap [6]. The laser resonator was formed by a spherical ($R \approx 5$ m) highly reflecting mirror on a copper substrate coated with gold and by a flat output mirror on a ZnSe substrate with the reflectance 65%. The distance between the resonator mirrors mounted on the end flanges of the chamber was 500 mm.

Figure 1 shows the scheme of the electrode unit of the laser (its design is described in [5]). The planes in which anode – cathode plate pairs were located made the angle $\alpha = 12^\circ$ with the optical axis of the laser. For such an arrangement of electrode plates, the size d of the projection of the plasma region of the pump discharge on the plane perpendicular to the optical axis of the laser is equal to ~ 6 mm. It is this size that determines the laser beam width.

The pump source of the laser based on the $C-C$ scheme (Fig. 1) and the power supply of the laser were similar to those used in [5]. The storage capacitor was $C_s = 3.6$ nF. The laser was powered by using a pulsed power supply, the two groups of peaking capacitors being arranged symmetrically with respect to the discharge gap. The electric parameters of the discharge were measured by two ohmic

A.V. Andramanov, D.D. Voevodin, A.V. Vysotskii, S.A. Kabaev, B.V. Lazhintsev, V.A. Nor-Arevyan, A.V. Pisetkaya, V.D. Selemir
Russian Federal Nuclear Center, All-Russian Research Institute of Experimental Physics, prosp. Mira 37, 607190 Sarov, Nizhnii Novgorod region, Russia; e-mail: lazhintsev@ntc.vniief.ru

Received 13 February 2009; revision received 7 July 2009
Kvantovaya Elektronika **39** (12) 1102 – 1106 (2009)
Translated by M.N. Sapozhnikov

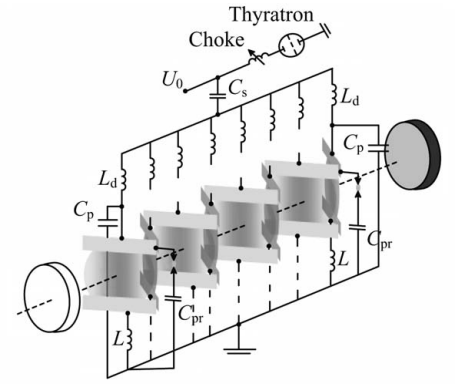

Figure 1. Electrode unit of the CO_2 laser and the pump source circuit: (L_d) decoupling inductance; (L) constructive inductance; (C_p) peaking capacitor; (C_{pr}) preionisation capacitor; (C_s) storage capacitor; (U_0) charging voltage.

dividers and two identical low-inductive flat current shunts. The dividers were connected directly to cathode and anode plates. The potential of the anode plate did not coincide with the Earth potential because of the constructive inductance L, and that is why the active resistance of the discharge was measured with the help of the second divider. The shunts were located on the sides of the discharge chamber, one of them being used in the common circuit of the pump and preionisation discharge, and another – in the thyratron circuit.

After the achievement of the breakdown voltage across peaking capacitors, a volume discharge was produced in the interelectrode gap. The discharge region width b between each pair of the electrode plates was ~ 1.3 mm, which corresponds to rather high values of the specific electric energy and power introduced to the discharge plasma.

Figure 2 presents the shapes of voltage pulses across the discharge gap, current pulses in the pump and preionisation discharge circuit, and the laser pulse.

The readings of the shunts and divider were mutually correlated during charging the peaking capacitor both in the discharge formation regime and in the absence of breakdown in the laser chamber, and also during discharging the storage capacitor in the discharge formation regime. According to the charge conservation law, the integral of the charge-exchange current of the storage and peaking capacitors measured with the help of the shunt is equal to a charge appeared on the peaking capacitor, measured with the divider, while the integral of the current during discharging the storage capacitor is equal to the initially accumulated charge. The charges determined in this way from oscillograms coincided with an accuracy of 5 % – 10 %.

The rise front of the voltage pulse before the discharge gap breakdown was ~ 40 ns and its maximum amplitude was ~ 11.3 kV. The duration and maximum amplitude of the discharge current pulse were ~ 25 ns and ~ 3.4 kA, respectively. In the oscillogram of the current pulse the shunt records the charging current of preionisation capacitors before the appearance of current in the pump discharge circuit. Figure 3 presents the calculated time dependence of the electric power P supplied to the plasma discharge. It follows from this calculation that for a charging voltage of 22 kV, no more than 0.35 J of electric energy is supplied to the discharge plasma, while the energy in the first peak of the current pulse, which most likely determines the output energy, does not exceed 0.28 J.

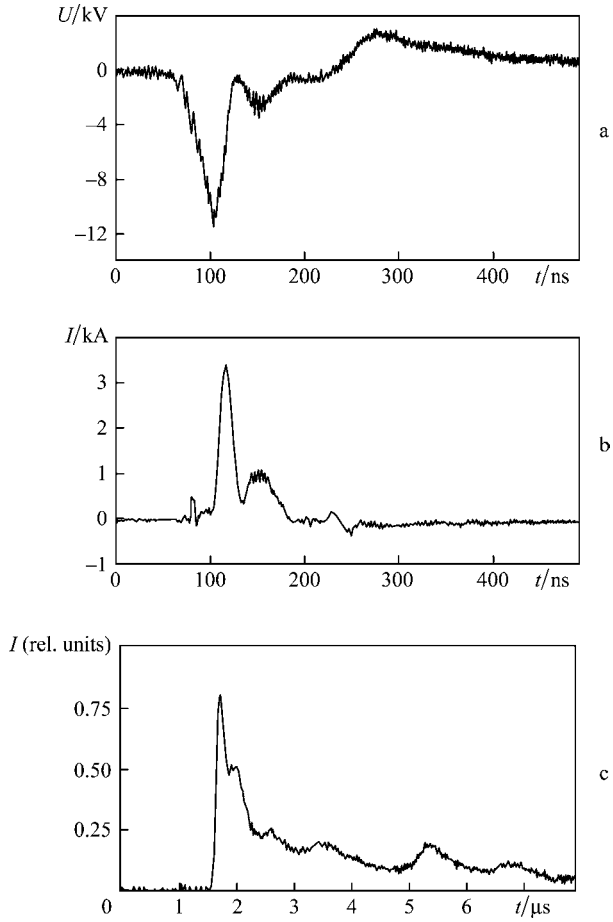

Figure 2. Oscillograms of voltage pulses across the discharge gap (a), current in the pump and preionisation circuit (b), and a laser pulse (c). The active mixture composition is $CO_2:N_2:He = 32:32:96$ Torr, the charging voltage is $U_0 = 22$ kV.

As shown in [7], the distributions of the energy density supplied to the active medium of the laser and the emission intensity of the discharge plasma in the visible spectral region are close in shape. The integrated emission of the discharge was measured and processed as in [5]. The widths of the emission intensity distribution of the discharge in the middle part of the discharge gap at the $0.1I_{max}$ and $0.5I_{max}$ levels were 6 and 3.5 mm, respectively.

Figure 4 presents the imprint of a laser beam on a photographic paper on which the reduced (approximately

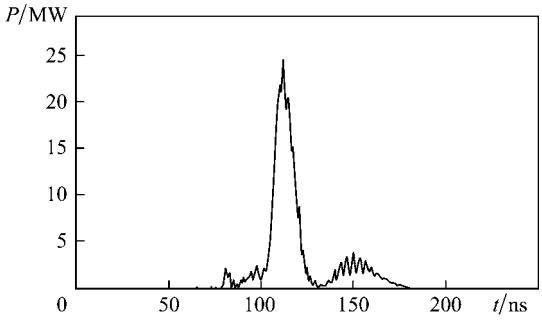

Figure 3. Time dependence of the power supplied to the discharge plasma. The active mixture composition is $CO_2:N_2:He = 32:32:96$ Torr, the charging voltage is $U_0 = 22$ kV.

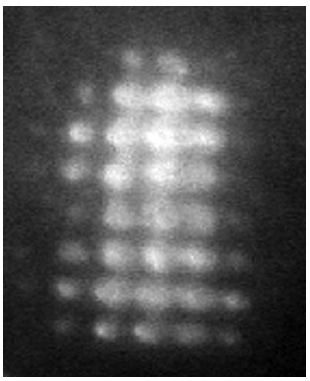

Figure 4. Laser beam imprint on a photographic paper. The spacing of a grid located in the near zone is 1 mm. The active mixture composition is $CO_2:N_2:He = 32:32:96$ Torr, $U_0 = 22$ kV.

seven times) image of the output laser mirror was projected. To simplify the interpretation of experimental results, a wire grid with a spacing of 1 mm was mounted near the output resonator mirror. The laser beam cross section was $\sim 6\times 8$ mm. One can see from Fig. 4 and the processed photograph of the integrated emission of the discharge that the imprint of the laser beam coincides in size with the discharge emission distribution only in the horizontal plane, whereas the imprint size in the vertical direction is smaller. This is explained by diffraction losses near electrodes in the case of formation of the caustics of the optical resonator at small gains.

To determine the degree of uniformity of the energy input over the length of the plate electrode, we studied the uniformity of emission of the discharge plasma between plate electrodes. Against the background uniform emission over the electrode length we observed diffusion columns 'related' to cathode spots. The diffusion columns appear when the rest of the energy stored in the storage capacitor is supplied to the discharge during the second peak of the current pulse.

During the propagation of laser radiation in the resonator of a laser with plate electrodes oriented at a considerable angle to the optical axis of the resonator, the radiation is amplified only in local regions occupied by the discharge plasma. The volume $V = hdl$ of the discharge gap of the plate-electrode laser is ~ 18 cm^3, whereas the real volume of the pump discharge plasma is only ~ 3 cm^3. Lasers with plate or conventional (solid) electrodes can be compared by the value of the averaged specific energy input $W_{sp} = E_p/V$ in the active medium, which determines the averaged gain and, correspondingly, the possible parameters of the laser.

Thus, the maximum specific pump power P_{sp} supplied to the discharge plasma at the atmospheric pressure of the active medium in the plate-electrode CO_2 laser is ~ 7 MW cm^{-3}, which considerably exceeds characteristic values $P \leqslant 0.2$ MW cm^{-3}, for example, in [1]. For the active medium at pressures used in experiments, the specific energy was ~ 450 J dm^{-3} atm^{-1}, which also exceeds the values 100–200 J dm^{-3} atm^{-1} that are typical for repetitively pulsed lasers studied, for example, in [1, 2]. Despite the large specific energy input to the discharge plasma, the average energy input to the discharge gap volume of the laser remains rather small (no more than 70 J dm^{-3} atm^{-1}).

The delay of the laser pulse with respect to the pump discharge current pulse as a function of the voltage across the storage capacitor is 1.3–1.8 μs. The full width at half-maximum of the first peak of the laser pulse is ~ 500 ns for the compositions and pressures of the working medium studied. The slowly decreasing part of the laser pulse consists of a few peaks of the total duration ~ 4 μs (see Fig. 2c). The peak output power achieves ~ 60 kW for the charging voltage 22 kV. Lasing is developing for a long time because the gain averaged over the discharge gap length is relatively small and the optical resonator has a low Q factor. The gain depends both on the average energy input to the discharge gap volume of the laser and the efficiency of this energy transfer to the laser levels of the CO_2 molecule.

We studied the energy characteristics of the laser at a low pulse repetition rate for the active mixture of compositions $CO_2:N_2:He = 1:1:3$, $CO_2:N_2:He = 1:2:5$, and $CO_2:N_2:He = 2:1:3$. The working pressure of the mixture was varied from 140 to 200 Torr. The optimal pressure for all compositions of the active mixture at which maximum energies were obtained was ~ 160 Torr.

Figure 5 presents the dependences of the laser radiation energy on the charging voltage for different compositions of the active medium. The maximum output energy of 15.9 mJ with the lasing efficiency 1.7 % (with respect to the energy stored in the storage capacitor) was obtained in the $CO_2:N_2:He = 1:1:3$ mixture at a pressure of 160 Torr and a charging voltage of 22 kV.

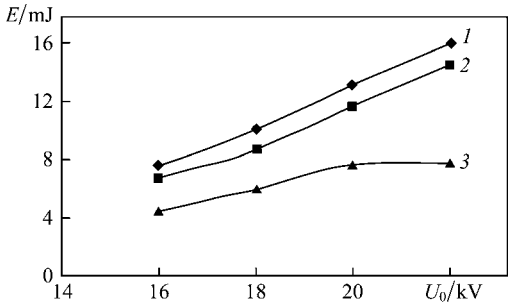

Figure 5. Dependences of the laser radiation energy on the charging voltage for active mixtures $CO_2:N_2:He = 32:32:96$ Torr (*1*); $CO_2:N_2:He = 20:40:100$ Torr (*2*) and $CO_2:N_2:He = 53:27:80$ Torr (*3*).

The low lasing efficiency is determined by several reasons. The charging voltages of the storage capacitor were too high for pressures of the active medium of the CO_2 laser under study. As a result, the reduced electric field strengths during the supply of the electric energy to the discharge exceed by several times the optimal value for the CO_2 laser [8]. This is explained by the fact that the high-voltage pump source, which was earlier used in a chemical laser [5], in conjunction with a resonance-diode charging circuit can provide a pulse repetition rate of 3–4 kHz at the storage energy level ~ 1 J only at high charging voltages.

In addition, the reflectance of the output mirror for the pump energies and active-medium lengths used in experiments should be considerably increased [1, 2]. Thus, the electrode plates were initially oriented at an angle of 30° to the optical axis of the laser [5], which provided the maximum lasing efficiency of only 1.3 %. In this case, due to a wider lasing region ($d = 10$ mm), the averaged gain was even smaller.

The processing of the oscillograms showed that the main part of the energy (0.22–0.28 J for charging voltages 16–22 kV) is supplied to the discharge plasma during the

first peak of the current pulse. Approximately the same energy is transferred from the storage to peaking capacitor by the onset of formation of a volume discharge, which amounts to 30 % – 45 % of energy stored in the storage capacitor. Thus, the laser efficiency with respect to the energy supplied to the discharge is 3 % – 5 %. In the absence of breakdown in the laser chamber, 65 % – 70 % of the stored energy is transferred to the peaking capacitor.

The radiation energy E_N of a packet consisting of a few tens of pulses was measured with a calorimeter in the high-repetition-rate lasing regime. Then, the average energy $E_{av}(f) = E_N(f)/N$ of one radiation pulse was determined for different repetition rates. The maximum pulse repetition rate $f_{0.8}$ obtained in experiments is the frequency at which the average pulse energy is ~ 80 % of energy in the low-repetition-rate regime.

In some experiments the diametric fan motor operated in the forced regime for a short time. In this case, the gas flow rate in the interelectrode gap increased up to 20 – 20.5 m s^{-1}.

Figure 6 presents the average energy E_{av} normalised to the energy in the low-repetition-rate regime as a function of f in the forced operation regime of the fan motor for the charging voltage $U_0 = 22$ kV. For the $CO_2:N_2:He$ = = 20 : 40 : 100 Torr mixture, the value $f_{0.8} = 3500$ Hz was obtained, and for the $CO_2:N_2:He$ = 3 : 32 : 96 mixture – the value $f_{0.8} = 3000$ Hz.

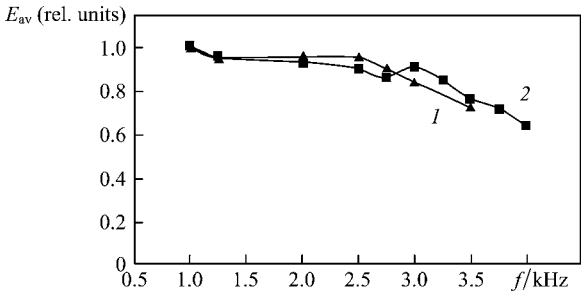

Figure 6. Dependences of $E_{av}(f)$ for $v \sim 20$ – 20.5 m s^{-1} and $U_0 = 22$ kV for active mixtures $CO_2:N_2:He$ = 32 : 32 : 96 Torr (*1*) and $CO_2:N_2:He$ = = 20 : 40 : 100 Torr (*2*).

The energy stability of laser pulses was measured for packets of 100 pulses at high repetition rates (a few kilohertz). A total packet of laser pulses was detected with an Ophir Nova II power meter and a PE10 pyroelectric sensor. The root-mean-square deviation σ of the pulse energy from its average value was calculated from measured pulse energies.

Figure 7 presents the dependences of σ on f for active-medium compositions $CO_2:N_2:He$ = 32 : 32 : 96 Torr and 20 : 40 : 100 Torr. The value of σ is ~ 55 % for $f \leqslant 2750$ Hz for both mixtures. As the repetition rate is increased, σ drastically increases. In the forced motor operation regime (up to the repetition rate 3000 Hz) and charging voltage $U_0 = 22$ kV for mixtures $CO_2:N_2:He$ = 32 : 32 : 96 Torr and 20 : 40 : 100 Torr, the value of σ did not exceed 5 % and 7 %, respectively.

The drastic increase in σ indicates the deterioration of the discharge homogeneity. This is explained by the appearance of strong fluctuations of the active-medium density caused by the 'preceding discharge', which remained partially in the discharge gap by the onset of the next discharge [3].

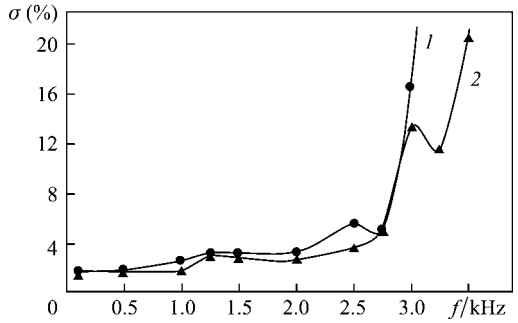

Figure 7. Dependences σ (f) for active mixtures $CO_2:N_2:He$ = = 32 : 32 : 96 Torr (*1*) and $CO_2:N_2:He$ = 20 : 40 : 100 Torr (*2*) for $U_0 = 22$ kV.

Figure 8 presents the dependences of σ on f for different gas flow rates. One can see that for each value of v there exists the limiting rate f_{lim} at which σ drastically increases. It is known that the gas flow rate determines the periodicity of the renewal of a gas mixture in the discharge gap by the onset of the next pulse, which is often characterised by the gas replacement coefficient K [1, 3]. For lasers in which the discharge in the active medium is produced by using massive electrodes, this coefficient is $K = v/(fd)$, where d is the width of the discharge region, which virtually coincides with the laser beam width. The stable high-repetition-rate regime in electric-discharge lasers is usually obtained for $K > 2.5$ [1, 3]. When the electrode plates are oriented at angle α to the optical axis of the laser, two gas replacement coefficients can be considered. The coefficient $K_1 = v\cos\alpha/(fb)$ characterises the gas mixture renewal in the discharge-plasma region, i.e. it is determined by the projection of the width of the discharge-plasma region to the direction of the gas flow rate. The coefficient $K_2 = v/(fd)$ characterises the gas-mixture renewal in the discharge gap. The formation of a homogeneous discharge at the specified pulse repetition rate depends on the value of K_1. The value of K_2 is related to a distance downstream of the laser medium by which the regions of gas heated and expanded during the discharge will be replaced. As a result, in the most interesting case $K_2 \sim 1$ near the edge of the optical resonance of the laser located downstream the gas, optical inhomogeneities appear, which can deteriorate the lasing conditions. Note that for f_{lim} in these experiments, K_1 changes from 7.4 for $v = 5.6$ m s^{-1} down to 5.1 for $v = 19$ m s^{-1}, while K_2 changes from 1.6 to 1, respectively. The possibility of operating in the high-repetition-rate regime at $K_2 \sim 1$ instead of $K > 2.5$, which is typical for lasers with massive electrodes, illustrates the advantages of using plate electrodes in IR lasers.

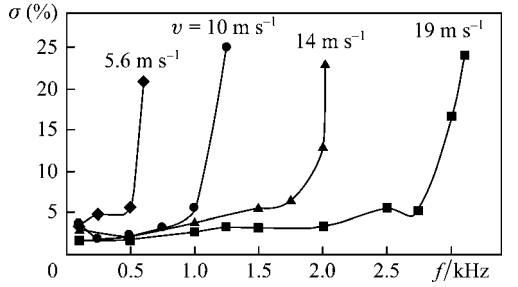

Figure 8. Dependences $\sigma(f)$ for different v and $U_0 = 22$ kV for the $CO_2:N_2:He$ = 32 : 32 : 96 Torr active mixture.

We observed in experiments the decrease in K_1 with increasing the gas flow rate and pulse repetition rate, which is not typical for electric-discharge lasers. First the region of gas heated in the discharge expands quite rapidly in the adiabatic process. Then, it continues to expand due to relatively slow convective heat exchange caused by strong turbulization of the gas flow. Note that at a distance of 0.5 mm from the axial line of each electrode plate downstream and upstream, the flow cross section changes by a factor of 1.5–2, producing strong turbulization of the flow. The time interval between discharges increases at low pulse repetition rates, which is accompanied by the increase in the size of heated-gas regions and the approach of their boundaries to the discharge gaps between each pair of electrode plates. This leads to the increase in the gas flow rate required to obtain a stable discharge at low pulse repetition rates, i.e. to the increase in K_1. It can be expected that the pulse repetition rate of the laser can be further increased by using mixtures with a higher concentration of helium and locating the preionisation unit upstream. Optical inhomogeneities appearing in the laser with $K_2 \sim 1$, which are caused by the incomplete removal of gas heated in the discharge from the optical resonator, require additional interferometric investigations.

3. Conclusions

The new design of the electrode unit allowed us to obtain the record high pulse repetition rate of 3000 Hz in the CO_2 laser for a comparatively low gas flow rate (9–20 m s^{-1}) in the interelectrode gap. The relative root-mean-square deviation of the pulse energy is within 5 %, and the near-field width of the laser beam is ~ 6 mm, which considerably exceeds the discharge width in the anode–cathode pair. For a specific pump power of ~ 7 MW cm^{-3} and a specific energy of ~ 450 J dm^{-3} atm^{-1}, the maximum output energy was 15.9 mJ for the technical efficiency 1.7 %. The average output power of the laser was ~ 40 W. We hope that the study of the electrotechnical parameters of the discharge and optimisation of the pump source will lead to the increase in the output energy and efficiency of the laser.

References

1. Hidekazu H., Katsumi M., Minoru O., Hideo T. *Rev. Sci. Instrum.*, **64**, 3061 (1993).
2. Klopper W., Bagrova K, du Pisania J., Ronander E., Meyer J.A. *Opt. Eng.*, **33**, 2866 (1994).
3. Borisov V.M., Vinokhodov A.Yu., Vodchits V.A., El'tsov A.V., Ivanov A.S. *Kvantovaya Elektron.*, **30**, 783 (2000) [*Quantum Electron.*, **30**, 783 (2000)].
4. Andramanov A.V., Kabaev S.A., Lazhintsev B.V., Nor-Arevyan V.A., Selemir V.D. *Kvantovaya Elektron.*, **35**, 311 (2005) [*Quantum Electron.*, **35**, 311 (2005)].
5. Andramanov A.V., Kabaev S.A., Lazhintsev B.V., Nor-Arevyan V.A., Pisetskaya A.V., Selemir V.D. *Kvantovaya Elektron.*, **36**, 235 (2006) [*Quantum Electron.*, **36**, 235 (2006)].
6. Andramanov A.V., Kabaev S.A., Lazhintsev B.V., Nor-Arevyan V.A., Selemir V.D. Russian Patent No. 2244990, from 10.04.03; *Izobreteniya*, (2), 610 (2005).
7. Andramanov A.V., Kabaev S.A., Lazhintsev B.V., Nor-Arevyan V.A., Pisetskaya A.V., Selemir V.D. *Kvantovaya Elektron.*, **35**, 359 (2005) [*Quantum Electron.*, **35**, 359 (2005)].
8. Mesyats G.A., Korolev Yu.D. *Usp. Fiz. Nauk*, **148**, 101 (1986).